SLAC-PUB-14250

Time-Resolved Pump-Probe Experiments at the LCLS

James M. Glownia,[1, 2,*] J. Cryan,[1,3] J. Andreasson,[4] A. Belkacem,[5] N. Berrah,[6] C. I. Blaga,[7] C. Bostedt,[8] J. Bozek,[8] L. F. DiMauro,[7] L. Fang,[6] J. Frisch,[8] O. Gessner,[5] M. Gühr, [1] J. Hajdu,[4] M. P. Hertlein,[10] M. Hoener,[6, 10] G. Huang,[10] O. Kornilov,[5] J. P. Marangos,[11] A. M. March,[12] B. K. McFarland,[1, 2] H. Merdji,[1, 13] V. S. Petrovic,[3] C. Raman,[14] D. Ray,[12, 15] D. A. Reis,[1, 2] M. Trigo,[1] J. L. White,[2] W. White,[8] R. Wilcox,[10] L. Young,[12]

R. N. Coffee, [1, 8] and P. H. Bucksbaum,[1, 2, 3]

[1]The PULSE Institute for Ultrafast Energy Science, SLAC National Accelerator Laboratory, 2575 Sand Hill Road, Menlo Park, CA 94025 USA

[2]Department of Applied Physics, Stanford University, Stanford, CA 94305 USA

[3]Department of Physics, Stanford University, Stanford, CA 94305 USA

[4]Laboratory of Molecular Biophysics, Department of Cell and Molecular Biology, Uppsala University, Husargatan, SE-75124, Uppsala, Sweden

[5]Ultrafast X-ray Science Laboratory, Chemical Sciences Division, Lawrence Berkeley National Laboratory, Berkeley, CA 94720 USA

[6]Department of Physics, Western Michigan University, Kalamazoo, MI 49008 USA

[7]The Ohio State University, Department of Physics, Columbus, OH 43210 USA

[8]The Linac Coherent Light Source, SLAC National Accelerator Laboratory, Menlo Park, CA 94025 USA

[9]Louisiana State University, Baton Rouge, LA 70803 USA

[10]Lawrence Berkeley National Laboratory, Berkeley, CA 94720 USA

[11]Blackett Laboratory, Imperial College London, London UK

[12]Argonne National Laboratory, Argonne, IL 60439 USA

[13]CEA-Saclay, IRAMIS, Service des Photons, Atomes et Molecules, 91191 Gif-sur-Yvette, France

[14]School of Physics, Georgia Institute of Technology, Atlanta, GA 30332 USA

[15]Department of Physics, Kansas State University, Manhattan, KS 66506, USA

**jglownia@slac.stanford.edu*

Abstract: The first time-resolved x-ray/optical pump-probe experiments at the SLAC Linac Coherent Light Source (LCLS) used a combination of feedback methods and post-analysis binning techniques to synchronize an ultrafast optical laser to the linac-based x-ray laser. Transient molecular nitrogen alignment revival features were resolved in time-dependent x-ray-induced fragmentation spectra. These alignment features were used to find the temporal overlap of the pump and probe pulses. The strong-field dissociation of x-ray generated quasi-bound molecular dications was used to establish the residual timing jitter. This analysis shows that the relative arrival time of the Ti:Sapphire laser and the x-ray pulses had a distribution with a standard deviation of approximately 120 fs. The largest contribution to the jitter noise spectrum was the locking of the laser oscillator to the reference RF of the accelerator, which suggests that simple technical improvements could reduce the jitter to better than 50 fs.

References and links

1. Y. Ding, A. Brachmann, F.-J. Decker, D. Dowell, P. Emma, J. Frisch, S. Gilevich, G. Hays, Ph. Hering, Z. Huang, R. Iverson, H. Loos, A. Miahnahri, H.-D. Nuhn, D. Ratner, J. Turner, J. Welch, W. White, and J. Wu, "Measurements and simulations of ultralow emittance and ultrashort electron beams in the linac coherent light source," Phys. Rev. Lett. **102**(25), 254801 (2009).
2. P. Emma, R. Akre, J. Arthur, R. Bionta, C. Bostedt, J. Bozek, A. Brachmann, P. Bucksbaum, R. Coffee, F.-J. Decker, Y. Ding, D. Dowell, S. Edstrom, A. Fisher, J. Frisch, S. Gilevich, J. Hastings, G. Hays, Ph. Hering, Z. Huang, R. Iverson, H. Loos, M. Messerschmidt, A. Miahnahri, S. Moeller, H.-D. Nuhn, G. Pile, D. Ratner, J.

Work supported in part by US Department of Energy contract DE-AC02-76SF00515.

Rzepiela, D. Schultz, T. Smith, P. Stefan, H. Tompkins, J. Turner, J. Welch, W. White, J. Wu, G. Yocky, and J. Galayda, "First lasing and operation of an angstrom-wavelength free-electron laser," Nat. Photonics (to be published).

3. A. Brachmann, C. Bostedt, J. Bozek, R. Coffee, F.-J. Decker, Y. Ding, D. Dowell, P. Emma, J. Frisch, S. Gilevich, G. Haller, G. Hays, Ph. Hering, B. Hill, Z. Huang, R. Iverson, E. Kanter, B. Kraessig, H. Loos, A. Miahnahri, H.-D. Nuhn, A. Perazzo, M. Petree, D. Ratner, R. Santra, T. Smith, S. Southworth, J. Turner, J. Welch, W. White, J. Wu, and L. Young, J. M. Byrd, G. Huang, R. Wilcox, "Femtosecond operation of the LCLS for user experiments,**"** presented at the 1st International Particle Accelerator Conference IPAC'10, Kyoto, Japan, 23–28 May. 2010.
4. R. Santra, N. V. Kryzhevoi, and L. S. Cederbaum, "X-ray two-photon photoelectron spectroscopy: a theoretical study of inner-shell spectra of the organic para-aminophenol molecule," Phys. Rev. Lett. **103**(1), 013002 (2009).
5. L. Young, E. P. Kanter, B. Krässig, Y. Li, A. M. March, S. T. Pratt, R. Santra, S. H. Southworth, N. Rohringer, L. F. Dimauro, G. Doumy, C. A. Roedig, N. Berrah, L. Fang, M. Hoener, P. H. Bucksbaum, J. P. Cryan, S. Ghimire, J. M. Glownia, D. A. Reis, J. D. Bozek, C. Bostedt, and M. Messerschmidt, "Femtosecond electronic response of atoms to ultra-intense X-rays," Nature **466**(7302), 56–61 (2010).
6. J. P. Cryan, J. Glownia, J. Andreasson, A. Belkacem, N. Berrah, C. I. Blaga, C. Bostedt, J. Bozek, C. Buth, L. F. DiMauro, L. Fang, O. Gessner, M. Guehr, J. Hajdu, M. P. Hertlein, M. Hoener, O. Kornilov, J. P. Marangos, A. M. March, B. K. McFarland, H. Merdji, V. Petrovic, C. Raman, D. Ray, D. Reis, F. Tarantelli, M. Trigo, J. White, W. White, L. Young, P. H. Bucksbaum, and R. N. Coffee are preparing a manuscript to be called "Auger electron angular distribution of double core hole states in the molecular reference frame."
7. M. Hoener, L. Fang, O. Kornilov, O. Gessner, S. T. Pratt, M. Gühr, E. P. Kanter, C. Blaga, C. Bostedt, J. D. Bozek, P. H. Bucksbaum, C. Buth, M. Chen, R. Coffee, J. Cryan, L. DiMauro, M. Glownia, E. Hosler, E. Kukk, S. R. Leone, B. McFarland, M. Messerschmidt, B. Murphy, V. Petrovic, D. Rolles, and N. Berrah, "Ultra-intense X-ray induced ionization, dissociation and frustrated absorption in molecular nitrogen," Phys. Rev. Lett. **104**(25), 253002 (2010).
8. A. Zewail, "Femtochemistry: atomic-scale dynamics of the chemical bond," J. Phys. Chem. A **104**(24), 5660–5694 (2000).
9. A. L. Cavalieri, N. Müller, Th. Uphues, V. S. Yakovlev, A. Baltuska, B. Horvath, B. Schmidt, L. Blümel, R. Holzwarth, S. Hendel, M. Drescher, U. Kleineberg, P. M. Echenique, R. Kienberger, F. Krausz, and U. Heinzmann, "Attosecond spectroscopy in condensed matter," Nature **449**(7165), 1029–1032 (2007).
10. A. L. Cavalieri, D. M. Fritz, S. H. Lee, P. H. Bucksbaum, D. A. Reis, J. Rudati, D. M. Mills, P. H. Fuoss, G. B. Stephenson, C. C. Kao, D. P. Siddons, D. P. Lowney, A. G. Macphee, D. Weinstein, R. W. Falcone, R. Pahl, J. Als-Nielsen, C. Blome, S. Düsterer, R. Ischebeck, H. Schlarb, H. Schulte-Schrepping, Th. Tschentscher, J. Schneider, O. Hignette, F. Sette, K. Sokolowski-Tinten, H. N. Chapman, R. W. Lee, T. N. Hansen, O. Synnergren, J. Larsson, S. Techert, J. Sheppard, J. S. Wark, M. Bergh, C. Caleman, G. Huldt, D. van der Spoel, N. Timneanu, J. Hajdu, R. A. Akre, E. Bong, P. Emma, P. Krejcik, J. Arthur, S. Brennan, K. J. Gaffney, A. M. Lindenberg, K. Luening, and J. B. Hastings, "Clocking femtosecond X rays," Phys. Rev. Lett. **94**(11), 114801 (2005).
11. B. Steffen, V. Arsov, G. Berden, W. A. Gillespie, S. P. Jamison, A. M. MacLeod, A. F. G. van der Meer, P. J. Phillips, H. Schlarb, B. Schmidt, and P. Schmüser, "Electro-optic time profile monitors for femtosecond electron bunches at the soft x-ray free-electron laser FLASH," Phys. Rev. ST Accel. Beams **12**(3), 032802 (2009).
12. M. Krikunova, T. Maltezopoulos, A. Azima, M. Schlie, U. Frühling, H. Redlin, R. Kalms, S. Cunovic, N. M. Kabachnik, M. Wieland, and M. Drescher, "Time-resolved pump-probe experiments beyond the jitter limitations at FLASH," Appl. Phys. Lett. **94**(14), 144102 (2009).
13. R. Wilcox, J. M. Byrd, L. Doolittle, G. Huang, and J. W. Staples, "Stable transmission of radio frequency signals on fiber links using interferometric delay sensing," Opt. Lett. **34**(20), 3050–3052 (2009).
14. R. K. Shelton, S. M. Foreman, L.-S. Ma, J. L. Hall, H. C. Kapteyn, M. M. Murnane, M. Notcutt, and J. Ye, "Subfemtosecond timing jitter between two independent, actively synchronized, mode-locked lasers," Opt. Lett. **27**(5), 312–314 (2002).
15. H. Tsuchida, "Timing-jitter reduction of a mode-locked Cr:LiSAF laser by simultaneous control of cavity length and pump power," Opt. Lett. **25**(19), 1475–1477 (2000).
16. J. Bozek, "AMO instrumentation for the LCLS X-ray FEL," Eur. Phys. J. Spec. Top. **169**(1), 129–132 (2009).
17. W. C. Wiley, and I. H. McLaren, "Time of flight mass spectrometer with improved Resolution," Rev. Sci. Instrum. **26**(12), 1150–1157 (1955).
18. D. Rolles, Z. D. Pešić, M. Perri, R. C. Bilodeau, G. D. Ackerman, B. S. Rude, A. L. D. Kilcoyne, J. D. Bozek, and N. Berrah, "A velocity map imaging spectrometer for electron-ion and ion-ion coincidence experiments with synchrotron radiation," Nucl. Instrum. Methods Phys. Res. B **261**(1-2), 170–174 (2007).
19. H. Stapelfeldt, and T. Seideman, "Colloquium: Aligning molecules with strong laser pulses," Rev. Mod. Phys. **75**(2), 543–557 (2003).
20. B. Kempgens, A. Kivimaki, M. Neeb, H. M. Köppe, A. M. Bradshaw, and J. Feldhaus, "A high-resolution N 1s photoionization study of the N_2 molecule in the near-threshold region," J. Phys. At. Mol. Opt. Phys. **29**(22), 5389–5402 (1996).
21. R. Wetmore, and R. Boyd, "Theoretical investigation of the dication of molecular nitrogen," J. Phys. Chem. **90**(22), 5540–5551 (1986).

22. Y. H. Jiang, A. Rudenko, M. Kurka, K. U. Kühnel, Th. Ergler, L. Foucar, M. Schöffler, S. Schössler, T. Havermeier, M. Smolarski, K. Cole, R. Dörner, S. Düsterer, R. Treusch, M. Gensch, C. D. Schröter, R. Moshammer, and J. Ullrich, "Few-photon multiple ionization of N2 by extreme ultraviolet free-electron laser radiation," Phys. Rev. Lett. **102**(12), 123002 (2009).
23. E. Gagnon, P. Ranitovic, X.-M. Tong, C. L. Cocke, M. M. Murnane, H. C. Kapteyn, and A. S. Sandhu, "Soft X-ray-driven femtosecond molecular dynamics," Science **317**(5843), 1374–1378 (2007).
24. P. Franceschi, D. Ascenzi, P. Tosi, R. Thissen, J. Zabka, J. Roithová, C. L. Ricketts, M. De Simone, and M. Coreno, "Dissociative double photoionization of N_2 using synchrotron radiation: appearance energy of the N^{2+} dication," J. Chem. Phys. **126**(13), 134310 (2007).
25. S. Krinsky, and Y. Li, "Statistical analysis of the chaotic optical field from a self-amplified spontaneous-emission free-electron laser," Phys. Rev. E Stat. Nonlin. Soft Matter Phys. **73**(6), 066501 (2006).
26. U. Frühling, M. Wieland, M. Gensch, T. Gebert, B. Schütte, M. Krikunova, R. Kalms, F. Budzyn, O. Grimm, J. Rossbach, E. Plönjes, and M. Drescher, "Single-shot terahertz-field-driven X-ray streak camera," Nat. Photonics **3**(9), 523–528 (2009).

1. Introduction

Significant advances have been made over the last ten years in the development of sub-picosecond x-ray free-electron lasers (xFEL), which can resolve and track atomic motion within molecules during a photo-chemical reaction. One such xFEL, the Linac Coherent Light Source (LCLS) at the SLAC National Accelerator Laboratory lies at the forefront, producing pulses shorter than ten femtoseconds with peak x-ray powers of up to 10 gigawatts, and pulse energies over 1 mJ in the range from 500 eV to more than 9 keV, pulse widths of several hundred to less than 10 fs, and pulse repetition rates from 30 Hz to 120 Hz [1–3]. The LCLS is the world's first hard x-ray laser with photon energies in the keV regime making it an excellent tool to study femtosecond molecular dynamics with atomic site specificity [4].

The first user commissioning operations of the LCLS in the fall of 2009 concentrated on atomic [5] and molecular [6,7] spectroscopy. These experimental campaigns included the first time-resolved x-ray/optical and optical/x-ray pump-probe experiments, which were performed on molecular N_2. Most ultrafast experiments rely on pump-probe techniques, in which dynamics are initiated by a short laser "pump" pulse and the evolution of the dynamics is probed by a second "probe" pulse after a variable time delay. The time resolution of measurements is limited by the temporal jitter between the two pulses, which can reach the attosecond domain if the pump and probe are derived from the same laser by means of a beam-splitter and path-length delay lines [8,9]. The situation is much more difficult when synchronizing physically dissimilar lasers that are not optically synchronized such as an amplified Ti:Sapphire laser and a xFEL.

The first level of synchronization uses conventional feedback techniques to stabilize the laser pulse arrival time relative to the radio frequency (RF) that drives the accelerator. This has lead to a timing stability of better than 1 picosecond (ps) at the LCLS. However, at a linear accelerator, the electron pulses arrival times exhibit an inherent timing "jitter" relative to the accelerator RF due to a number of factors: Thermal fluctuations can change the dimensions of the accelerator; noise and drift in the RF distribution network also affect the synchronization. Energy jitter in the electrons converts to timing jitter in the magnetic chicane compressors. All of these residual timing shifts can be overcome by directly measuring the time of arrival of the electrons relative to the RF. This was done at SLAC and at the German electron synchrotron laboratory (DESY) in earlier experiments utilizing nonlinear mixing of the laser radiation with the transient electric field of the electrons. Electro-optic (EO) sampling measured the electron bunch arrival times relative to a synchronized external laser. Re-timing the data based on the measured arrival times then gave sub-100 fs timing resolution even though the actual temporal jitter was hundreds of femtoseconds [10–12].

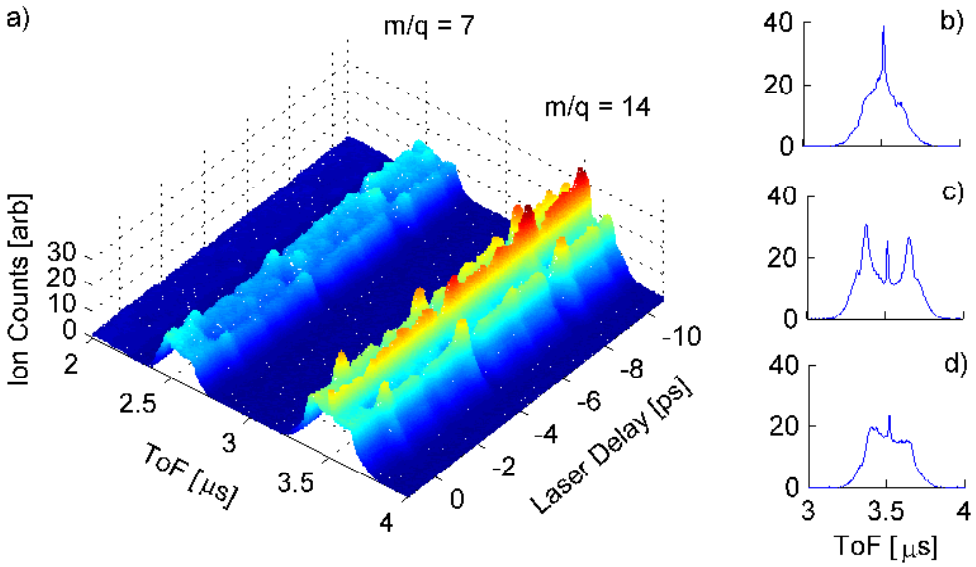

Fig. 1. , Pump-probe time-delay dependent ion time-of-flight (ToF) spectra of molecular nitrogen. (a) ToF spectrum near m/q = 14 and m/q = 7, where m and q are the mass and charge, respectively, of the ion fragment. Negative delay indicates that the optical pulse precedes the x-ray pulse. Periodic rotational alignment features are clearly visible in all peak structures. The inset plots show line-outs of the m/q = 14 ToF spectrum at various laser delays: t = −8.5 ps (b) nitrogen molecules anti-aligned with respect to the spectrometer axis, t = −8.0 ps (c) nitrogen molecules aligned along spectrometer axis, and t = 1 ps (d) x-ray pulse precedes laser pulse (no alignment).

The LCLS has developed an alternative but similar solution based on two resonant RF phase cavities (PCAV-1 and PCAV-2). These resonant cavities measure the electron bunches as they pass through on their way to the electron dump just after the laser undulator. A reference harmonic of the phase cavity is then used to lock the optical laser source to the average arrival time of the electron bunch. Single-shot phase analysis of these same phase cavities provides a measure of the single-shot bunch arrival time.

The electron synchronization is necessary but not sufficient to ensure synchronization of laser/x-ray pump/probe pulses in LCLS experiments. In this study, we used ultrafast molecular processes with sub-10 fs x-rays and sub-100 fs optical laser pulses to analyze the synchronization in this setup. In the optical pump/x-ray probe geometry, we induced impulsive molecular alignment initiated by the optical laser. Photoionization of neutral N2 by an ultrafast LCLS x-ray pulse induced Coulomb explosion of the molecule producing singly and multiply charged fragments that were observed in an angle-apertured ion time-of-flight spectrometer (Fig. 1a-d). In the x-ray pump/optical probe geometry, we observed the IR laser-triggered dissociation of x-ray produced quasi-bound N_2^{2+} dications. We find the long term timing jitter between the x-ray and optical pulses to be 280 fs full width at half-maximum (FWHM), or 120 fs root-mean-squared deviation (RMS).

In this paper we first present the measured electron timing information and show how this data is used to synchronize the optical laser with the electron bunch time arrival times. We then show the results of several pump-probe experiments performed at the LCLS and provide some insight into the relative timing stability between the x-ray and optical laser pulses.

2. Timing the electrons

The electron bunch arrival time (BAT) signal at the LCLS undulator hall was measured with two S-band, 2805 MHz, resonant cavities (PCAV-1 & 2) excited by the passing electron bunch. The periodic electric field induced in the RF has a phase that is related to the arrival

time of the electron bunch. This phase was compared to the known phase of a stabilized frequency reference running at 476 MHz, and this difference was used to derive the BAT with respect to the stabilized RF source. Software feedback periodically adjusted the phase of the 476 MHz reference to match the average measured beam arrival times to compensate for long term drifts. The drift-corrected 476 MHz broadcast signal from this oscillator was transmitted over an interferometrically stabilized fiber distribution system to a receiver in the Laser Hall that locks the laser to this RF source.

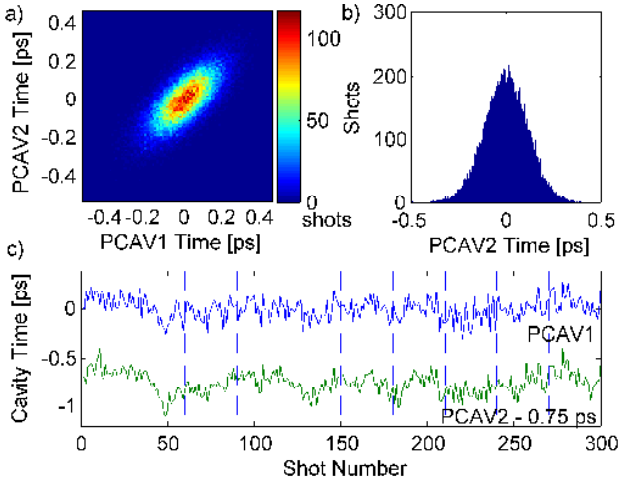

Fig. 2. , Electron bunch arrival time data for a typical run. (a) Histogram of measured BATs for both phase cavities. (b) Histogram of BATs for phase cavity two showing the BATs in more detail and a standard deviation of ~112 fs. (c) Time series plots of both phase cavities for successive shots while the machine was running at 30 Hz. The blue trace shows the measured BAT times for phase cavity one while the green trace shows the measured BAT times for phase cavity two (displaced by 0.75 ps for clarity). The dashed lines denote one second intervals. We see that over these short time scales the standard deviation of either cavity is ~100 fs.

Figure 2a shows the single-shot bunch arrival times for the two phase cavities for over 55 thousand consecutive LCLS pulses. The running mean values are used to re-synchronize the optical laser at ~1 second intervals. The variation of the BATs from the mean therefore indicates the shot-to-shot temporal jitter in the x-ray arrival time with respect to the 476MHz RF distribution. It was found in post processing the data that the software used to determine the phase of the first RF cavity had an intermittent phase wrapping problem due to a miscalibration for the low bunch charges that were used. The phase wrapping caused intermittent noise to be added to some of the shots for this cavity. This noise both broadens the observed timing uncertainty and skews the timing correlation plot above. This lack of correlation limited their use to improve the overall timing system response. These technical problems have now been resolved, and this situation is therefore expected to improve. We show a histogram of the measured raw BATs from the most stable phase cavity (PCAV-2) in Fig. 2b. This histogram indicates that the arrival time of the e-beam jitters with a standard deviation of about 112 fs (FWHM of 260 fs). However, this jitter includes both short term and long term drifts in the accelerator. Since the laser is locked to the electron beam timing at ~1 second intervals the jitter over this time scale is more relevant than the overall jitter. The measured BAT times from PCAV-2 plotted over successive one second time intervals is shown in Fig. 2c. On this shorter time scale the e-beam jitter has a standard deviation of ~100 fs which demonstrates that the long term drifts in the timing system are well compensated. Thus, the inherent uncorrected standard deviation (root-mean-square) jitter present in the machine is on the order of 100 fs.

The BAT signals can be used in post-processing to correct the timing values on a shot-by-shot basis, similar to the use of electro-optic timing measurements at the SLAC Sub-Picosecond Pulsed Source (SPPS) and the Hamburg VUV free electron laser facility (FLASH). In this case, the synchronization hardware and software are capable of sub-50 fs RMS errors [3]. This is the current best case precision of the arrival of the electron bunch relative to the RF.

3. Timing the laser

The optical laser is synchronized by a stabilized fiber optic timing system described in Ref [13]. This system locks a mode-locked Ti:Sapphire oscillator to the 476 MHz RF reference derived from resonant RF cavities. This synchronizes the laser oscillator to the average electron bunch arrival time. The Ti:Sapphire amplifier and the transport and optical elements to the experiment are not contained within the feedback loop.

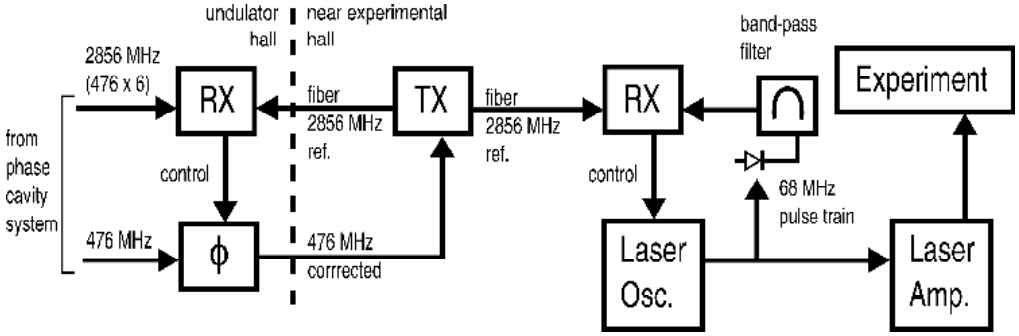

Fig. 3. , LCLS near experimental hall laser timing system. A signal derived from the average electron beam time of arrival measured in the undulator hall is transmitted through a stabilized fiber system and used to synchronize the optical laser oscillator in the near-experimental hall that is hundreds of feet away. The oscillator pulses are then amplified, converted to beam rate, and transported to the experiment and timing jitter from these processes are not compensated by the timing system.

Figure 3 shows how timing information passes through the system. The phase cavity system provides both 2856 MHz and 476 MHz signals whose spectral phases change according to the bunch arrival time. The timing transmitter (TX) in the Near-Experimental Hall (NEH) sends 2856MHz reference signals over optical fiber to two receivers, one in the undulator hall near the phase cavities and one near the Ti:Sapphire oscillator in order to synchronize the two receivers with each other. Each receiver (RX) is a phase comparator between two RF inputs: the fiber reference signal; and either a photodiode harmonic signal of the same frequency, or an RF reference from the phase cavity system. In the scheme of Fig. 3, the comparison made at the undulator hall receiver between the 2856 MHz signal from the phase cavity and a 2856 MHz reference from the NEH transmitter controls the 476MHz RF sent back to the transmitter. This resynchronizes the reference 2856 MHz from the NEH transmitter to the phase cavity signal. Thus the receiver near the laser is also in synchronization with the phase cavity signal since it receives the updated reference RF from the transmitter. The receiver near the laser compares the reference with an RF signal derived from the 68MHz pulse train emitted from the mode-locked laser oscillator. A photodiode feeds a band-pass filter that transmits the harmonic signal at 476MHz. This is multiplied by six to produce a signal at 2856MHz, which is compared to the reference. The phase difference is used to generate a control signal that drives a piezo-electric actuated end-mirror in the Ti:Sapphire oscillator to keep the laser synchronized to the reference RF, i.e., synchronized to the average bunch arrival time measured by the phase cavity system. We used an additional adjustable laser-to-reference phase signal to add arbitrary phase to the locking loop in order to

achieve simultaneous arrival of the laser and the x-rays in the experimental region without the use of long optical delay lines.

The bandwidth of the timing synchronization system is limited to approximately 800 Hz. This is primarily due to the mass of the oscillator cavity end mirror as well as the capabilities of the piezo-electric actuators. This relatively small bandwidth has a profound impact on the control system's ability to compensate for in-loop jitter. The time averaged in-loop jitter is measured by observing the drift in the difference between the 476 MHz harmonic of the oscillator diode and the RF reference that is locked to the electron BAT times. With a 1 kHz measurement bandwidth the time averaged in-loop jitter is about 25 fs RMS, which shows that low frequency contribution to the overall jitter is well compensated by the 800 Hz system bandwidth. However, at a > 10 kHz measurement bandwidth the time averaged jitter grows to be 120 fs RMS, demonstrating that a significant degree of uncompensated jitter is present in the system. This can perhaps be compensated for in the future by using a large-bandwidth cavity mirror or to slightly modulate the oscillator laser pump power since both of these techniques have been used in the past to achieve sub 1 fs timing jitter in oscillators over relatively wide bandwidths in other systems [14,15].

4. Experiment and results

The first pump-probe experiment used to commission the timing system at LCLS was the study of x-ray ionization and dissociation of laser-aligned molecular nitrogen [6]. The laser is used to impulsively align the molecules via rotational Raman scattering approximately ~8.4 ps prior to the x-ray pulse, and the width of the alignment revival feature requires the laser and x-rays to be synchronized to better than 400 fs. Moreover, the physics of x-ray absorption in N_2 also leads to transient effects that can be used to test the synchronization at a level of approximately 75 fs.

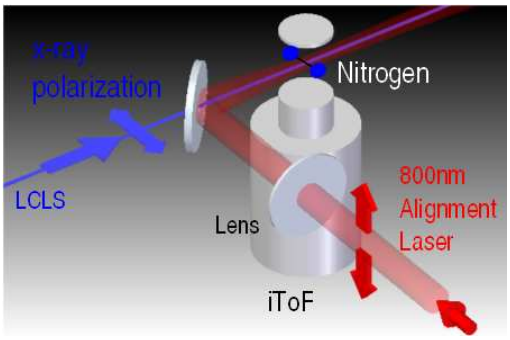

Fig. 4. , Experimental setup showing nitrogen molecules aligned along the iToF axis. The 800 nm alignment laser impulsively aligns molecules along its polarization. X-rays from the LCLS then dissociate these molecules. Nitrogen ions that are emitted towards the repeller plate are directed back towards the iToF, resulting in a time delay difference between these ions and those that are emitted towards the iToF initially.

The experiment was performed at the AMO end station of the LCLS [16]. The experimental setup is sketched in Fig. 4. Supersonic expansion of nitrogen with a backing pressure of 3 bar through a 100 µm diameter nozzle and a 200 µm diameter skimmer produced a molecular beam. The target volume contained a nearly uniform molecular density of ~10^{13} cm^{-3} and the target gas had a rotational temperature of approximately 20 K. The 800 nm laser pulse used to align the molecular gas had a pulse energy of ~400 µJ, a repetition rate of 360 Hz, and a duration of ~60 fs in a quasi-flat top pulse, which was measured by autocorrelation after the experimental run. It was not possible to obtain direct optical autocorrelation information at the interaction region during the run. The pulse could have been as long as 75 fs due to imperfections in the optical path and dispersion in the intra-

vacuum optics. The LCLS x-ray pulses had approximately 10^{11} photons per pulse, a photon energy of ~1050 eV, a repetition rate of 30 Hz, and a focal area of roughly 3 μm^2 as measured by optical damage tests.

The ions were detected at the 30 Hz LCLS beam rate in a standard ion time-of-flight (iToF) apparatus [17,18] that was usually operated in Wiley-McLaren configuration with a ~150V/cm extraction field. The iToF extractor electrode contained a 1 x 10 mm slit oriented orthogonal to the incident x-ray direction. The iToF axis was perpendicular to both the x-ray polarization and the molecular beam. A 500 mm lens located just outside the vacuum chamber focused the optical laser to a ~75 µm diameter spot. This beam was combined with the x-rays in a co-propagating geometry using a dielectric mirror with a 2mm central hole for the x-rays. The residual transmitted optical light was collected with an identical dielectric mirror and imaged on a CCD camera for remote inspection of the position at the focal volume. We estimate a peak optical intensity of ~5 x 10^{13} W/cm^2 in the target volume, which at the target gas rotational temperature of 20K is predicted by our simulations to give a degree of alignment corresponding to $\langle cos^2(\theta) \rangle$~0.7. We varied the relative optical/x-ray delay with an optical delay line with a 1 µm (6.6 fs) position precision. Typical scans consisted of ~1000 x-ray pulses per time step where each x-ray pulse produced roughly 30 ion counts on the detector. A typical time delay scan is shown in Fig. 1.

The synchronization of the aligning laser "pump" and the x-ray laser "probe" was determined in several steps, which was completed within two hours. First, photoionization of molecular nitrogen by both beams in the overlap region provided a coarse ~1ns timing signal for this adjustment. Once the coarse timing was completed we moved the optical laser pulse to be early with respect to the x-ray pulse. In this configuration the optical laser could impulsively align the nitrogen along the laser's polarization direction [19]. The x-rays at later times then photo-dissociated the molecules and the ion fragments were detected. For dissociating nitrogen molecules aligned along the detector axis, as shown in Fig. 4, the extracting field collects both fragments, but their opposite momenta lead to different ion paths and different arrival times at the detector. The width of these two iToF distributions indicates the degree of alignment. The atomic ion fragments from dissociating molecules aligned perpendicular to the detector axis are mostly blocked by the slit aperture in the extractor electrode, and therefore do not contribute to the ion signal. The transient alignment repeats at the fundamental rotational revival period of 8.4 psec, and the revivals continue for nanoseconds.

Figure 5a shows the pump-probe time delay dependent iToF spectrum in the vicinity of m/q = 14. The central region of the peak has strong contributions from the quasi-bound molecular nitrogen dication, N_2^{++}. The broader peaks on each side represent dissociating singly charged atoms, whose momenta toward or away from the detector are recorded by negative or positive ToF differences relative to the peak center, respectively. The variation of the spectrum with time delay shows the effect of laser-induced alignment, as follows: Negative time delays correspond to the arrival of the optical laser pulse before the x ray pulse. At these times the optical laser can impulsively align the ensemble. The peak alignment occurs approximately 200 fs following the laser pulse. This process is easily observed in Fig. 5 as a significant increase in the size of the peak wings. A detailed plot of the molecular alignment near the half revival is shown in Fig. 5b. The molecular alignment was observed by dividing the integrated wing region by the integrated central portion of the m/q = 14 (N^+ or N_2^{++}) feature. This value is sensitive to the molecular alignment since molecular dissociation is fast compared to the rotational timescale in our experiment (axial recoil approximation). Ions that are emitted nearly parallel to the spectrometer axis in either forward (towards the detector) or backward (away from the detector) direction form the wings of the iToF peak, and they travel the shortest and longest distances, respectively. A preferential alignment of the molecules along the spectrometer axis in the moment of inner-shell photoionization directly translates into an enhancement of the iToF peak wings compared to the center

portion. This effect is strongly enhanced by the narrow slit aperture in the ion spectrometer. The periodic revival structure shown in Fig. 1 and Fig. 5b results from the free evolution and rephasing of rotational wave packets that were produced by the optical laser. The steepest feature corresponds to a rapid change from alignment to anti-alignment at the half revival, at a delay of approximately 4.25 ps. A computer simulation of the rotational revival structure using the experimental parameters has good qualitative agreement with the data, confirming a peak alignment of $<cos^2(\theta)>$~0.7. Additionally, when the iToF data were re-binned using the electron BAT data from PCAV-2 as a reference, there was a slight improvement in the measurement fidelity (Fig. 5b red curve). The alignment and anti-alignment peaks are better resolved with time re-binning and the peaks become smoother which is expected from molecular alignment, and 50 fs is the shortest time bin that makes any significant improvement of the alignment signal. Such re-binning could be used at the LCLS in the future to increase the temporal fidelity of pump probe experiments.

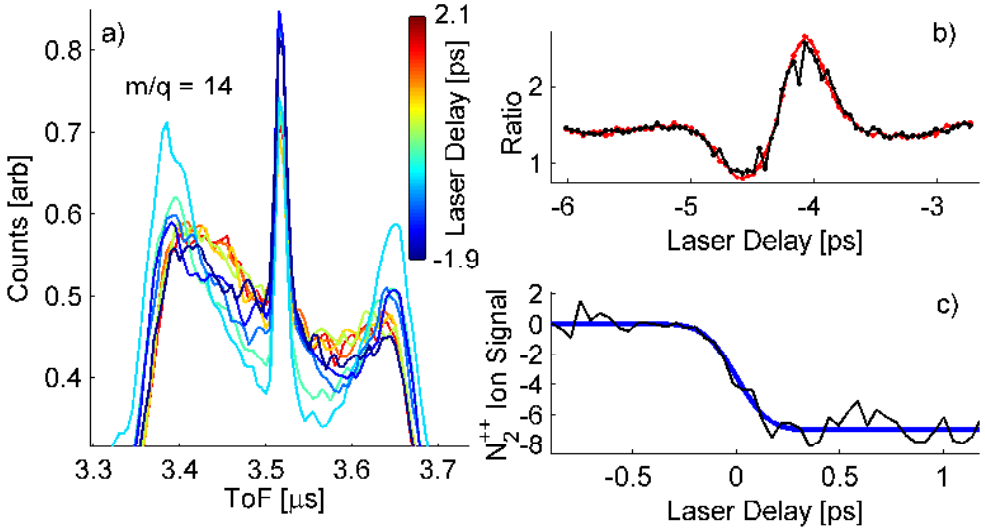

Fig. 5. , The ion ToF spectrum. (a) The N_2^{++} molecules appear as a sharp central feature in the m/q = 14 peak in this spectrum while the dissociated atomic ions are displaced by the momentum imparted by coulomb explosion. When the optical laser pulse succeeds the x-ray pulse (positive delays), the N_2^{++} fraction is decreased by strong-field induced dissociation of the dication. Transient molecular alignment along and perpendicular to the spectrometer axis leads to alternating enhancement in the peak wings and peak center. (b) The black curve is the trace of the ratio of the integrated N^+/N_2^{++} peak wings to the integrated central portion showing detailed molecular alignment structure near the molecular half revival. The red curve is a time re-binned data set using ~50 fs time bins showing improvement in the signal fidelity. (c) N_2^{++} center peak intensity vs. pump-probe time delay (black) after subtraction of atomic N^+ signal contributions (see text). Strong-field dissociation of N_2^{++} by optical pulses that succeed the x-ray pulse allows for a direct determination of the apparatus function and time zero by a corresponding drop in the N_2^{++} intensity. The blue curve is a Gaussian error function fit to the data with a FWHM of 283 fs that is expected to be dominated by the timing jitter between the laser and the x-rays.

We determined the x-ray/optical apparatus function and the position of zero delay time by observing a different physical process in which the roles of pump and probe are reversed: the dissociation of x-ray-produced N_2^{++} by an intense optical field. The formation of the nitrogen dication by x-ray core-level ionization and subsequent Auger relaxation (the so-called KLL process) occurs in the Auger relaxation lifetime of 6.4 fs [20]. This is the photoabsorption process that has the highest cross section at our x-ray photon energy of 1050 eV. The molecular dication has several long-lived "quasi-bound" metastable states [21–24], and produces a sharp spectral feature in the center of the m/q = 14 iToF peak as depicted in Fig. 5.

If the intense optical laser comes *after* the x-ray pulse rather than before it, the laser can efficiently dissociate the dication into two nitrogen ions, either through resonant absorption or non-resonant predissociation. This produces an observable decrease in the N_2^{++} peak in the iToF spectrum (Fig. 5c). Simulations of the self-amplified stimulated emission (SASE) process at LCLS operating in a low bunch charge mode show that the x-ray pulse envelope used in the study presented here is less than 10 fs [1–3], and likely to be shorter than the N_2 Auger decay time scale of approximately 6 fs. Any pump-probe cross-correlation is therefore dominated by the much longer optical pulse duration, ~75fs, and by the timing jitter between the x-ray and optical laser pulses.

5. Discussion

The N_2^{++} signal is partially obscured by a substantial background of dissociating atomic ions, and this background is strongly dependent on the alignment of the molecular ensemble. To isolate the contributions from the dication, it was necessary to remove the dynamic effects of the alignment. The alignment signal is also apparent in the manifold of doubly ionized atoms at m/q = 7 (see Fig. 1a), and we used this to calibrate the background subtraction. The doubly charged atomic ions are mostly generated by core-ionization of molecules followed by Auger relaxation and dissociation into a doubly charged and neutral atomic fragment. This produces one ion in the iToF detector. The background process in the N_2^{++} peak is ionization and Auger relaxation that leads to two singly charged fragments, and two counts in the detector. To correct for this background, we subtracted 1.8 times the baseline subtracted central N^{++} signal from the baseline subtracted N_2^{++} signal. The fact that the multiplication factor is not exactly two is primarily due to the unequal branching ratios for producing the two ions as well as detector nonlinearities, and the factor of 1.8 provides the best fit between the alignment data around the quarter and half revivals. The resultant "corrected" central N_2^{++} peak is shown as a function of laser delay in Fig. 5c. We observe a step function that we associate with the temporal overlap of the x-ray pulse and the laser pulse. The step location is consistent with the onset of the molecular alignment. A Gaussian error function was fit to the step feature and the related Gaussian was found to have a FWHM of 283 fs (120 fs RMS). We believe that this is an accurate representation of the timing jitter between the optical laser pulse and the x-ray pulse, and this value is consistent with the uncompensated in-loop jitter from the laser system.

6. Conclusion

We have analyzed the timing performance of the LCLS x-ray free electron laser using the first x-ray-optical pump-probe experiments at the LCLS. We have probed the field-free impulsive molecular alignment of a diatomic molecule, N_2, demonstrating the feasibility of using ultrafast optical lasers to align gas phase targets at ultrashort pulse x-ray sources. Furthermore, our analysis of the ionization and dissociation of N_2 shows that timing synchronization between the optical and x-ray lasers can be achieved with precision better than 280 fs FWHM. However, the short pulse duration of LCLS, which is estimated to be less than 10 fs under some operating conditions, create an opportunity and a need for improved timing in the future. We believe that the main limiting factor in controlling the timing jitter was uncompensated jitter from the laser system and associated optical delay lines. This jitter can be corrected in post processing by measuring the optical laser beam arrival times at the experiment on a single shot basis or by increasing the bandwidth of the timing synchronization system. Our analysis shows that the jitter could be improved to better than 50 fs if the electron BAT jitter were reduced to the electronic limit using existing techniques, and this timing information along with accurate laser time of arrival information could possibly push the overall time resolution down towards 50 fs. However, an important additional source of jitter in xFEL's comes from the nonlinear x-ray generation process, which can change the position of the x-ray pulse relative to the peak electron current [25]. Techniques for dealing

with this have been proposed recently [26]. An ideal timing system would clock both the x-rays and the laser shot by shot basis using a single physical process in a pump probe geometry, similar to this experiment, but with very short timing resolution over several hundred fs.

Acknowledgments

The authors would like to thank Rick Iverson, Paul Emma, Zhirong Huang, and Yuantao Ding for their work in achieving sub-10fs xFEL pulses. This research is supported through the PULSE Institute at the SLAC National Accelerator Laboratory by the U.S. Department of Energy, Office of Basic Energy Sciences. RC receives primary support through the LCLS at SLAC by the U.S. Department of Energy. OK, OG and AB were supported by the Director of Science, BES, Chemical Sciences Division of the U.S. DOE under contract No. DE-AC02-05CH11231. LFD and CIB were supported under contract DE-FG02-04ER15614 by the U.S. Department of Energy. VP was funded by the NSF under grant PHY-0649578. MH, LF and NB are funded by DOE-BES under contract DE-FG02-92ER14299. MH thanks the Alexander von Humboldt Foundation for his Feodor Lynen fellowship. AMM and LY were supported by the Chemical Sciences, Geosciences, and Biosciences Division of the Office of Basic Energy Sciences, Office of Science, US Department of Energy, under Contract No. DE-AC02-06CH11357. JA thanks The Swedish Foundation for International Cooperation in Research and Higher Education (STINT).